Combustion and Flame 211 (2020) 124–132

Contents lists available at ScienceDirect

Combustion and Flame

journal homepage: www.elsevier.com/locate/combustflame

Experimental and modeling study of benzaldehyde oxidation

Sylvain Namysl[a], Matteo Pelucchi[b], L. Pratali Maffei[b], Olivier Herbinet[a], Alessandro Stagni[b], Tiziano Faravelli[b], Frédérique Battin-Leclerc[a,*]

[a] Laboratoire Réactions et Génie des Procédés, CNRS-Université de Lorraine, 1 rue Grandville, 54000 Nancy, France
[b] Department of Chemistry, Materials and Chemical Engineering "G. Natta ", Politecnico di Milano, P.zza Leonardo da Vinci 32, 20133 Milano, Italy

ARTICLE INFO

Article history:
Received 3 July 2019
Revised 11 August 2019
Accepted 18 September 2019
Available online 4 October 2019

Keywords:
Jet-stirred reactor
Benzaldehyde
Phenyl radical
Oxidation

ABSTRACT

Benzaldehyde is an aromatic aldehyde commonly considered in bio-oil surrogate formulation, and an important intermediate in the oxidation of other aromatic reference fuels such as toluene. However, its oxidation has never been previously investigated experimentally and no product formation profiles were reported in the very limited pyrolysis studies available in the literature. In this study, the gas-phase oxidation of benzaldehyde was investigated in a jet-stirred reactor. 48 species were detected using gas chromatography, mainly CO, CO_2 and phenol. The important formation of CO and phenol indicates a rapid formation of phenyl radicals. This was confirmed by a kinetic analysis performed using the current version of the CRECK kinetic model, in which the reactions of phenyl radicals and oxygenated aromatic compounds have been updated.

1. Introduction

Benzaldehyde is the lightest aromatic aldehyde and is one of the major intermediates in the combustion and atmospheric oxidation of benzyl radical [1]. For this reason, its formation and consumption pathways are accounted for in detailed kinetic models for the combustion of toluene and heavier aromatic compounds (e.g. [2–4]). Furthermore, many oxygenated aromatic compounds are formed during the decomposition of biomass [5,6] and aromatic aldehydes (e.g. furfural and derivatives or hydroxybenzaldehydes (see Fig. 1a) and methoxybenzaldehydes) are a non-negligible part of these products [5,6].

Oxygenated aromatic compounds (phenol, anisole, catechol, guaiacol, vanillin) are gaining academic and industrial interest due to their presence in bio-oils produced from biomass fast pyrolysis [2,7,9]. Therefore, the influence of different functional groups on their combustion properties should be systematically addressed. Moreover, the impact of oxygenated aromatics on PAHs and soot growth should be better analyzed, as the high aromatic content of bio-oils could lead to undesired increased formation of particulate matter [10]. The purpose of this study is to better assess the combustion kinetics of benzaldehyde (see Fig. 1b), and also to propose a first overview towards an improved understanding of the oxidation of oxygenated aromatics with multiple substitutions of interest as bio-oil surrogates (e.g. vanillin) [7].

Benzaldehyde pyrolysis has already been studied in batch reactors by Hurd and Bennet [11] and by Solly and Benson [12] covering a temperature range from 573 K to 963 K at atmospheric pressure. Pyrolysis experiments have also been carried out in flow reactors by Grela et al. [13] at high temperatures (1005–1270 K) and low-pressure ($P = 0.01$ kPa), by Bruinsma et al. [14] at atmospheric pressure and over a temperature range from 773 K to 1173 K, and by Vasiliou et al. [8] between 1200 K and 1800 K and pressures ranging from 0.1 to 0.2 kPa. These studies showed that benzaldehyde decomposes to give phenyl radical plus H atom and CO: $C_6H_5CHO \rightarrow C_6H_5CO + H \rightarrow C_6H_5 + CO + H$, contrary to the usual aliphatic aldehydes where the alkyl acyl bond is the weakest (R-CHO) (see Fig 1c). However none of these studies provided mole fraction profiles for the fuel or the decomposition products for benzaldehyde pyrolysis. Also to our knowledge no oxidation study has been reported in the literature at present.

The aim of this study is to propose a first detailed set of data for the oxidation of benzaldehyde in a jet-stirred reactor (JSR) coupled with gas chromatographs (GCs). Using different type of detectors coupled to gas chromatography, mole fractions profiles were obtained for benzaldehyde and 48 of its products. These profiles were then used to update the benzaldehyde oxidation subset in the current version (1902) of the CRECK kinetic model.

* Corresponding author.
E-mail address: frederique.battin-leclerc@univ-lorraine.fr (F. Battin-Leclerc).

https://doi.org/10.1016/j.combustflame.2019.09.024

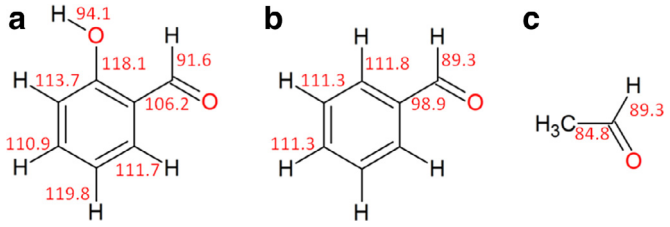

Fig. 1. Structures of a) 2-hydroxybenzaldehyde, b) benzaldehyde and c) acetaldehyde. Bond dissociation energies are given at 298 K and in kcal mol^{-1} (references: a) et b) [7] and c) [8]).

2. Experimental methods

The JSR used for the experiments has often been used for kinetic studies of pyrolysis [15] and combustion [16]. It consists of a fused silica sphere (volume 92 cm^3) equipped with four injection nozzles positioned in a cross located at the center of the sphere. This injection method ensures high turbulence in the reactor and leads to homogeneity in gas phase concentration. A quartz annular preheating zone, in which the temperature of the gas is progressively increased up to the reactor temperature, precedes the reactor inlet and is responsible for the homogeneity in gas phase temperature.

The gas residence time inside the annular preheater is very short compared to its residence time inside the reactor (a few percent), so as to limit undesired reactivity in this section. The heating is ensured by resistances (Thermocoax) rolled around the reactor and around the preheating zone, which allows flexibility and swiftness in the heating of each area. Temperatures are measured by K-type thermocouples located in a glass finger inside the inlet cross (for the reaction temperature measurement) and between the resistances and the external wall of the reactor (for the temperature control of each zone). The reaction temperature is assumed to be equal to that measured in the inlet cross according to the isothermal reactor hypothesis, with a maximum gradient of ±5 K.

Benzaldehyde was provided by Sigma Aldrich with a purity of 99%. He (99.999% pure) and O_2 (99.999%) were provided by Messer. Gas flow rates are controlled by mass flow controllers and the liquid flow rate by a Coriolis flow controller followed by a vaporization chamber maintained 10 K above benzaldehyde boiling temperature. The relative uncertainty in the flow measurements is around 0.5% for each controller, thus about 2% on the residence time.

The outlet gas leaving the reactor is then transported by a short heated line to GCs. The first GC, equipped with a Carbosphere packed column, a thermal conductivity detector (TCD) and a flame ionization detector (FID), is used for the quantification of light-weight compounds like methane, carbon monoxide and carbon dioxide. The second GC, fitted with a Q-Bond capillary column and a FID preceded by a methanizer, is used for the quantification of compounds containing from 2 carbon atoms, like acetylene or ethylene, to compounds with 5 carbon atoms (e.g. cyclopentadiene). The methanizer (nickel catalyst for hydrogenation) allows to detect species like CO and CH_3CHO with a better sensitivity. A third GC equipped with a HP-5 capillary column and an FID is used for the detection of the heaviest compounds. Products like benzene, benzaldehyde, phenol, naphthalene or biphenyl are quantified with this apparatus. The identification of reaction products is performed using a GC equipped with both types of capillary columns and coupled to a mass spectrometer (quadrupole) with ionization at 70 eV. Calibrations are performed by injecting standards when it is possible with a maximum relative error in mole fractions around ±5% and ±10% for the other species calibrated using the effective carbon number method. Concerning fuel calibration, as benzaldehyde properties are at the limit of the experimental set-up abilities, the error in the fuel measurements can be estimated to ±10%, despite the direct calibration. Experimental mole fraction data in a spreadsheet are reported in the Supplementary Material attached to this study.

Benzaldehyde oxidation was studied between 700 K and 1100 K at 107 kPa, at three equivalence ratios: $\varphi = 0.5–1–2$. The residence time in the reactor was fixed at 2 s and the inlet mole fraction of fuel was 0.5%. Helium was used as the inert gas. For each experiment, the carbon mass balance has been calculated and is estimated to be ≈90% of the global inlet of carbon atoms.

3. Kinetic model

The CRECK model adopted in this work (466 species and 16,263 reactions) implements a $C_0–C_3$ core subset obtained by coupling the H_2/O_2 and C_1/C_2 from Metcalfe et al. [17], C_3 from Burke et al. [18], and heavier fuels from Ranzi et al. [19,20]. It covers reactions from syngas to heavy diesel fuel pyrolysis and combustion, including PAH formation [2] as well as a new subset of reactions for oxygenated aromatics of interest as bio-oil surrogate components [7]. The thermochemical properties for species not specifically belonging to the benzaldehyde subset were adopted, when available, from the ATcT database of Ruscic [21] or from Burcat's database [22]. For the species involved in the benzaldehyde subset and not already implemented in the CRECK mechanism, the properties have been determined with the software THERGAS [23] based on Benson group additivity method [24].

Table 1 shows the primary pyrolysis and oxidation reactions of benzaldehyde, highlighting modifications and new reaction pathways implemented in this study (reactions whose parameters were estimated or taken from literature). It is composed of 18 reactions classed into different reaction types. The kinetic parameters given are: A, the pre-exponential factor in $(cm^{-3}•mol^{-1})^{n-1}/s$ with n, the order of the reaction and Ea, the activation energy in cal/mol. Benzaldehyde can react through unimolecular initiations (reactions 1–2 in Table 1). The hypothesis has been made that only the aldehydic function is reactive and that the aromatic ring cannot react by its own. Due to the lack of specific kinetic information, kinetic parameters of initiation reactions have been determined based on bond dissociation energies (BDEs) as reported in Pelucchi et al. [7]. The enthalpies of formation of the radical involved in the BDE estimation are presented in SM.

Reactions 3–12 correspond to bimolecular initiations and H-abstraction reactions. Only the bimolecular reaction with oxygen has been taken into account. The kinetic parameters of the H-abstractions from the aldehydic position have been determined based on previous studies on linear aldehydes [25].

Ipso-addition reactions on the fuel are modeled by the reactions 13 to 17 and correspond to the additions of the main radicals onto the ring at the aldehydic position. The kinetic parameters of ipso-addition reactions have been determined based on the rate rules reported in [7]. Reactions with the aromatic hydrogen atoms were considered as negligible compared to those involving the aldehydic one.

Reaction 18 is the reaction of alpha-scission of the radical C_6H_5CO formed after the abstraction of the aldehydic hydrogen atom. The rate constant of reaction 18 has been adopted from Solly and Benson [12], as already proposed in the toluene model by Bounaceur et al. [26]. It should be noted that the value from Solly and Benson is the only high pressure limit determination available in the literature and most probably carries large uncertainties (i.e. one order of magnitude) mostly due to the very limited temperature range considered in the analysis (614–647 K). However, from a broader kinetic model perspective, the C_6H_5CO radical is very rapidly decomposed to phenyl radical and CO, without significant further interactions with the mixture. The addition of O_2 to

Table 1
Primary pyrolysis and oxidation reactions of benzaldehyde in cal, s, mol, cc units.

Reactions	*A*	*n*	*Ea*	References	No.
Unimolecular initiations					
$C_6H_5CHO=HCO+C_6H_5$	*5.00E+15*	*0.0*	*98,900.0*	CRECK [7]	(1)
$C_6H_5CHO=C_6H_5CO+H$	*3.00E+15*	*0.0*	*89,300.0*	CRECK [7]	(2)
Bimolecular initiations and H-abstractions					
$O_2+C_6H_5CHO=HO_2+C_6H_5CO$	*1.36E+07*	*2.0*	*41,405.9*	CRECK [7,25]	(3)
$OH+C_6H_5CHO=H_2O+C_6H_5CO$	*1.20E+10*	*1.0*	*−855.1*	CRECK [7,25]	(4)
$HO_2+C_6H_5CHO=H_2O_2+C_6H_5CO$	*3.20E+06*	*2.0*	*14,062.9*	Estimated [25]	(5)
$CH_3+C_6H_5CHO=CH_4+C_6H_5CO$	*2.40E+05*	*2.0*	*3516.3*	CRECK [7,25]	(6)
$H+C_6H_5CHO=H_2+C_6H_5CO$	*1.20E+07*	*2.0*	*2573.6*	Estimated [25]	(7)
$C_6H_5CHO+C_7H_7=C_7H_8+C_6H_5CO$	*1.08E+05*	*2.0*	*14,062.9*	CRECK [7,25]	(8)
$C_2H_5+C_6H_5CHO=C_2H_6+C_6H_5CO$	*1.60E+05*	*2.0*	*5128.0*	CRECK [7,25]	(9)
$C_6H_5+C_6H_5CHO=C_6H_6+C_6H_5CO$	*2.96E+08*	*1.0*	*867.9*	CRECK [7,25]	(10)
$C_5H_5+C_6H_5CHO=C_5H_6+C_6H_5CO$	*2.72E+05*	*2.0*	*12,129.8*	CRECK [7,25]	(11)
$C_6H_5CHO+C_6H_5O=C_6H_5OH+C_6H_5CO$	*1.44E+05*	*2.0*	*10,683.4*	CRECK [7,25]	(12)
Ipso-additions					
$C_6H_5CHO+O=C_6H_5O+HCO$	*4.00E+12*	*0.0*	*5000.0*	[27]	(13)
$C_6H_5CHO+CH_3=C_7H_8+HCO$	*1.50E+12*	*0.0*	*4000.0*	CRECK [7]	(14)
$C_6H_5CHO+C_2H_3=C_6H_5C_2H_3+HCO$	*1.20E+12*	*0.0*	*15,200.0*	CRECK [7]	(15)
$C_6H_5CHO+OH=C_6H_5OH+HCO$	*9.63E+13*	*0.0*	*19,228.0*	CRECK [7]	(16)
$C_6H_5CHO+H=C_6H_6+HCO$	*4.70E+12*	*0.0*	*8600.0*	CRECK [7]	(17)
Alpha-scission decomposition					
$C_6H_5CO=C_6H_5+CO$	*5.80E+14*	*0.0*	*23,000.0*	[12]	(18)

C_6H_5CO has also been investigated, based on acetaldehyde similar reactions. However, it was shown that these reactions were negligible and a decision was made to remove them from the mechanism.

The kinetic values of reactions 5 and 7 were already present in the mechanism, but their estimation needed a reevaluation due to deviations between the model computed results and the experimental data. Thus, their kinetic constants were decreased (within the estimated uncertainty) in order to better reproduce the fuel reactivity. The pre-exponential factors of reactions 5 and 7 have so been multiplied by factors of 0.5 and 0.3, respectively, with respect to the reference values for H-abstractions from the aldehydic moiety of linear aldehydes [25]. The adopted rate constant modifications are well within the uncertainty range of those parameters (a factor of 3). This uncertainty is established based on other parameters adopted in literature models [28]. In fact, Mendes et al. [29] declared an uncertainty of 2.5–3 based on the uncertainties of the single point energies. We considered a factor of 3 as an upper limit as uncertainties related to the treatment of anharmonicities and to the frequencies may also be present.

The OpenSMOKE++ package [30] has been used to perform all the kinetic simulations and analyses here presented.

4. Results and discussion

Figure 2 presents the experimental and simulated mole fraction profiles of benzaldehyde. Reported experimental error is ±5%, as discussed in Section 2. Benzaldehyde starts to react at 750 K and is completely consumed at 1025 K, except under fuel rich conditions.

It can be observed that the equivalence ratio has only a minor impact on the conversion of the fuel. The kinetic model reproduces the onset of reactivity well within the experimental uncertainty slightly overpredicting the fuel conversion between 850 and 950 K. It should be noted that the model exhibits a higher dependence on the equivalence ratio compared to the experimental measurements.

Figures 3 and 4 display the mole fraction profiles of O_2 and the main products obtained during the oxidation of benzaldehyde. Styrene, benzofuran and cresol experimental profiles do not fit with the simulated profiles on the same chart. Therefore, they have been adjusted in order to fit in the chart with the computed data (styrene and benzofuran data are multiplied by 10 and cresol profile divided by 25 under fuel rich conditions).

The 48 products have been identified during this study; they can be divided in three main categories (species in *italic* are only present under the form of traces, thus their profiles are not reported in Figs. 3 and 4):

- acyclic compounds: carbon monoxide, carbon dioxide, methane, acetylene, ethylene, ethane, propene, propyne, allene, acetaldehyde, acrolein, *acetone*, butenyne, 1,3-butadiene.
- cyclic oxygenated compounds: *cyclopentenone*, anisole, benzoquinone, phenol, benzofuran, *benzodioxol, hydroxybenzaldehyde*, cresol, *acetophenone, benzodioxol-2-one, methylbenzofuran, ethylphenol, cinnamaldehyde, diphenylether*, dibenzofuran, *indanone*.
- cyclic hydrocarbons: 1,3-cyclopentadiene, benzene, toluene, *ethylbenzene, xylene, phenylacetylene*, styrene, *cumene, methylstyrene, indene, methylindene, dihydronaphthalene*, naphthalene, biphenyl, *acenaphthylene*.

Due to our analytical set-up, the quantification of hydrogen and water is not possible. It can also be noticed that neither formaldehyde nor catechol were detected during the experiments. Co-elution problem for catechol and detection limits for formaldehyde could explain their absence amongst the detected

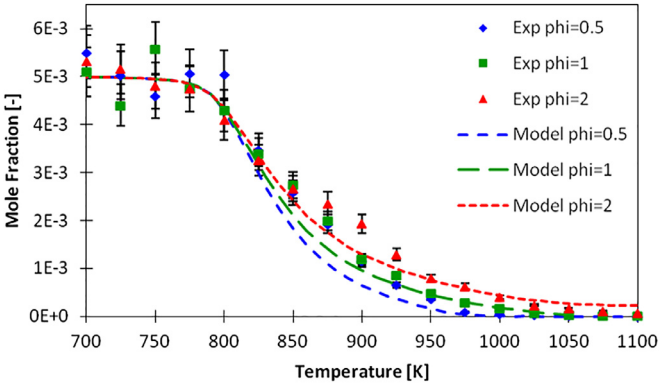

Fig. 2. Comparison between experimental (symbols) and predicted (lines) mole fraction profiles of benzaldehyde. Error bars are ±10%.

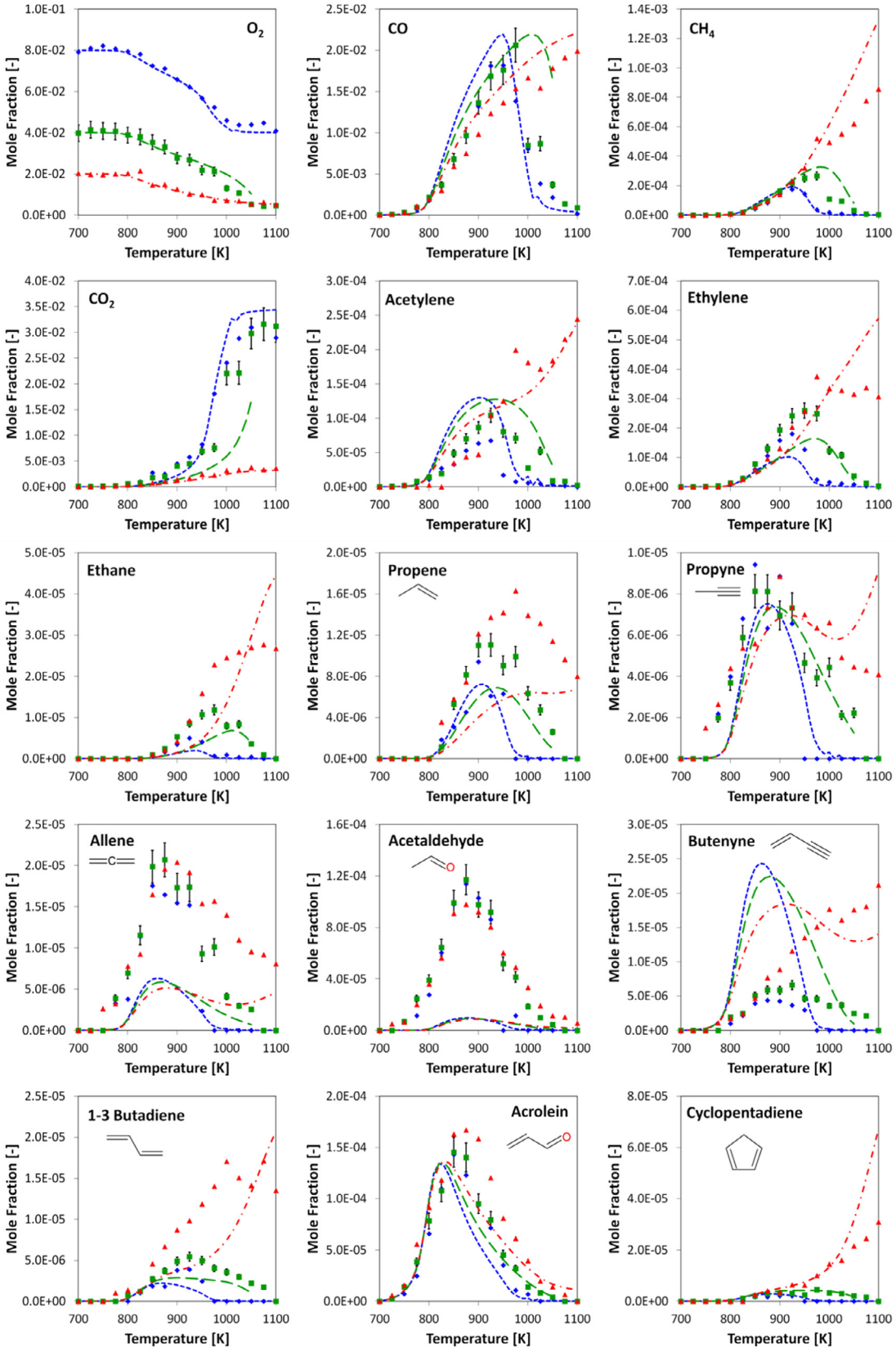

Fig. 3. Benzaldehyde oxidation in a jet-stirred reactor at $\varphi = 0.5$, 1 and 2, $p = 107$ kPa and $\tau = 2.0$ s. Comparison between experimental (symbols: ♦ $\varphi = 0.5$, ■ $\varphi = 1$, ▲ $\varphi = 2$) and predicted (lines: – – – $\varphi = 0.5$, ——— $\varphi = 1$, – · – · – $\varphi = 2$) mole fractions of O_2 and C_1–C_5 products. For clarity, error bars are only displayed for $\varphi = 1$ (±5% for O_2, CO, CO_2 and CH_4; ±10% for the others).

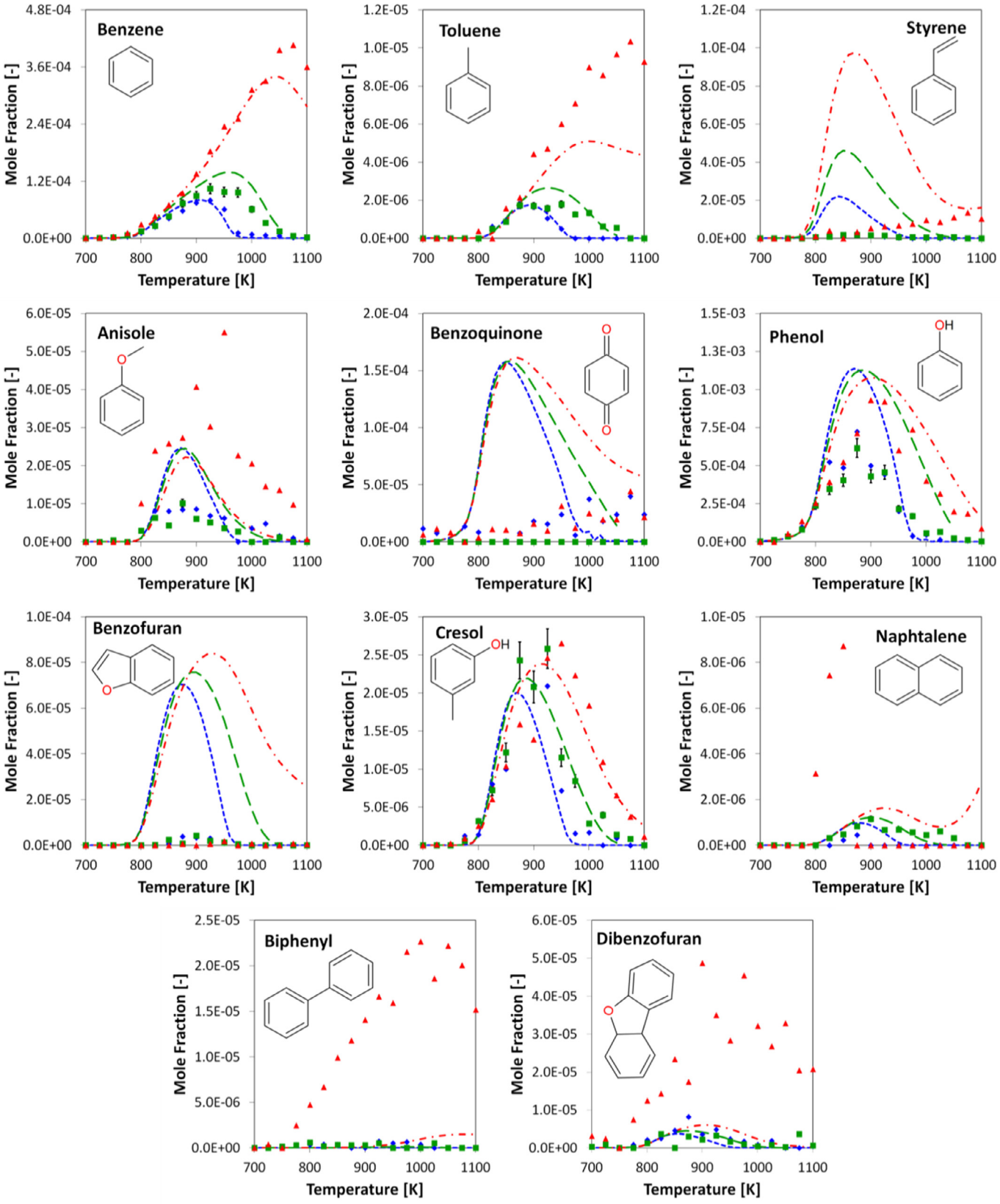

Fig. 4. Benzaldehyde oxidation in a jet-stirred reactor at $\varphi = 0.5$, 1 and 2, $p = 107$ kPa and $\tau = 2.0$ s. Comparison between experimental (symbols: ♦ $\varphi = 0.5$, ■ $\varphi = 1$, ▲ $\varphi = 2$) and predicted (lines: – – , $\varphi = 0.5$, — – , $\varphi = 1$, – · – , $\varphi = 2$) mole fractions of C_6+ products. For clarity, error bars are only displayed for $\varphi = 1$ (±10% for all the products).

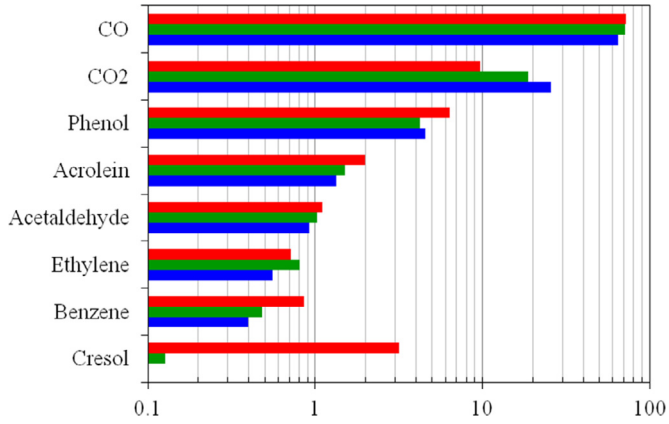

Fig. 5. Selectivity analyses at 850 K for the three equivalence ratios. ($\varphi = 0.5$, $\varphi = 1$, $\varphi = 2$).

products. Those products could have been expected due to the presence of methane and phenol in the gas phase with oxygen.

Figure 5 presents the product selectivity at 850 K for the three studied equivalence ratios. Carbon monoxide and carbon dioxide are the main products at this temperature. Phenol, acrolein, acetaldehyde and ethylene are the other main products formed. Cresol is a specific product of the fuel rich conditions. The overall agreement between the experimental and modeling data presented in Figs. 2, 3 and 4 is reasonable especially for equivalence ratios of 0.5 and 1.

At the highest temperatures (T>1000 K) under fuel rich conditions, model predictions are less accurate. The model predicts mole fractions of benzene and toluene lower than what is experimentally observed, which could lead to an overprediction of 1,3-cyclopentadiene, ethane, propyne and methane. The model also does not predict as much acetaldehyde as experimentally measured and estimates a production of catechol which was not observed experimentally. The profile of benzoquinone ($C_6H_4O_2$) is also overpredicted by the model.

Steady state numerical solutions were not found for stoichiometric conditions above 1050 K. The model predicts an oscillating behavior as frequently observed for smaller species [31]. However, a stable behavior was observed in the experiments.

Figure 6 shows a rate flux analysis of benzaldehyde oxidation at 850 K for stoichiometric conditions for a conversion of 50%. This conversion rate has been chosen in order to investigate the primary product decomposition pathways. For clarity, some species like CO and CO_2 are not shown. Under these conditions, benzaldehyde mainly reacts by the abstractions of the aldehydic hydrogen atom as suggested by Vasiliou et al. [8] for pyrolysis (89% at 850 K). This H-abstractions on the fuel leads to the formation of the C_6H_5CO radical, which quickly decomposes by alpha-scission in phenyl radical and carbon monoxide. The phenyl radical then leads to the phenoxy radical (C_6H_5O in Fig. 6). This radical is the precursor of almost all the products experimentally observed (e.g. acrolein, acetaldehyde, cresol…).

Benzaldehyde also reacts by ipso-addition reactions of hydrogen atom and C_2H_3 radical producing benzene and styrene. Styrene can then react through different H additions on different sites. An addition on the substituted unsaturation can lead to the formation of the radical $C_6H_5CHCH_3$ or to the formation of a radical C_6H_5 and ethylene. The radical $C_6H_5CHCH_3$ can also decompose into C_6H_5 radical and ethylene or can form the fuel back with the intervention of the radical HO_2. Styrene can also react by ipso-addition reactions to form benzene.

Benzene is formed by ipso-addition of H atom on benzaldehyde, styrene and phenol. Benzene is almost exclusively transformed into C_6H_5O via two pathways:

1) $O + C_6H_6 = H + C_6H_5O$ (97%)
2) $R + C_6H_6 = RH + C_6H_5$; $C_6H_5 + O_2 = C_6H_5O + O$ (1.4%)

Thus the formation and consumption of benzene is totally ruled by ipso-addition reactions on the other aromatic compounds present in the gas phase. As discussed in [27], the resonance stabilized phenoxy radical largely contributes to phenol formation by means of H-abstraction ($C_6H_5O + RH = C_6H_5OH + R$) on C_6H_5CHO and catechol and recombination with H atoms. Indeed 49% of the consumption flux of the radical C_6H_5 is dedicated to the formation of phenol. Phenol is then consumed in a significant fraction by H-abstraction reactions by O, OH, and HO_2 to give C_6H_5O radicals (18%). Therefore, a cycle phenol/phenoxy is exhibited by the mechanism and could be important in the overall reactivity of the system. This observation is also supported by the sensitivity analysis on benzaldehyde performed at 770 K under stoichiometric conditions and presented in Fig. 7. This temperature was chosen to investigate the reactions important at the start of the reactivity. Charts for other equivalence ratios are reported in the Supplementary Material attached to this study.

The most important reactions, promoting the reactivity, are the H-abstractions on the fuel by HO_2 and C_6H_5O to form the radical C_6H_5CO. This radical subsequently decomposes into C_6H_5 and C_6H_5O, also contributing to the phenol/phenoxy cycle.

Phenoxy radical (C_6H_5O) and the phenol/phenoxy cycle are controlling the reactivity at low temperatures. HO_2 radical has also an important impact as it is involved in the phenol/phenoxy cycle via the reaction: $HO_2 + C_6H_5O = O_2 + C_6H_5OH$. This analysis confirms that the C_6H_5O radical is the key intermediate in the reactivity of benzaldehyde at low-temperature. Thus its consumption, through the reactions $HO_2 + C_6H_5O => O_2 + C_6H_5OH$ and $O + C_6H_5O => 2CO + C_4H_5$, inhibits the reactivity. Furthermore, these reactions are consuming radicals by forming stable species (CO, O_2…) or by reducing the number of radical points in the system via termination reactions. Figure 8 presents a scheme of this analysis.

HO_2 also reacts with the fuel to give H_2O_2, giving two OH radicals and therefore accelerating the reactivity through a multiplication of the number of radicals. The chemistry of other intermediates like acrolein (C_2H_3CHO) and catechol phenoxy-like radical (RCATEC) have also a promoting effect on the reactivity, but less dominant. Concerning the other equivalence ratios, the same analysis has been performed and the results are very similar. This observation seems to confirm the fact that the equivalence ratio has a minor impact on the overall reactivity.

Acetaldehyde and acrolein are produced by the decomposition of C_6H_5O to C_4H_5 and CO through the reaction: $O + C_6H_5O => 2CO + C_4H_5$. Indeed the C_4H_5 radical reacts with oxygen to form HCO and acrolein: $O_2 + C_4H_5 => HCO + C_2H_3CHO$. Acrolein leads mainly to the formation of C_2H_3 radical (12.5%) via H-abstraction by OH, O, and H to give C_2H_3 and CO according to the lumped step $R + C_2H_3CHO => RH + CO + C_2H_3$. This lumped step corresponds to the abstraction of the aldehydic H-atom followed by a decarbonylation of the radical (R-C*=O) as discussed in [25]. C_2H_3 then decomposes into formaldehyde in a large amount (30%) via the addition of dioxygen. Acetaldehyde is formed by the addition-elimination reaction of OH radical on acrolein: $OH + C_2H_3CHO => HCO + CH_3CHO$ accounting for 3% of the consumption flux of acrolein. However the model is not able to predict the correct amount of acetaldehyde. This could also explain the overprediction of styrene mole fraction, due to an overproduction of C_2H_3 radicals from acrolein. Furthermore the model considers the formation of formaldehyde through the reac-

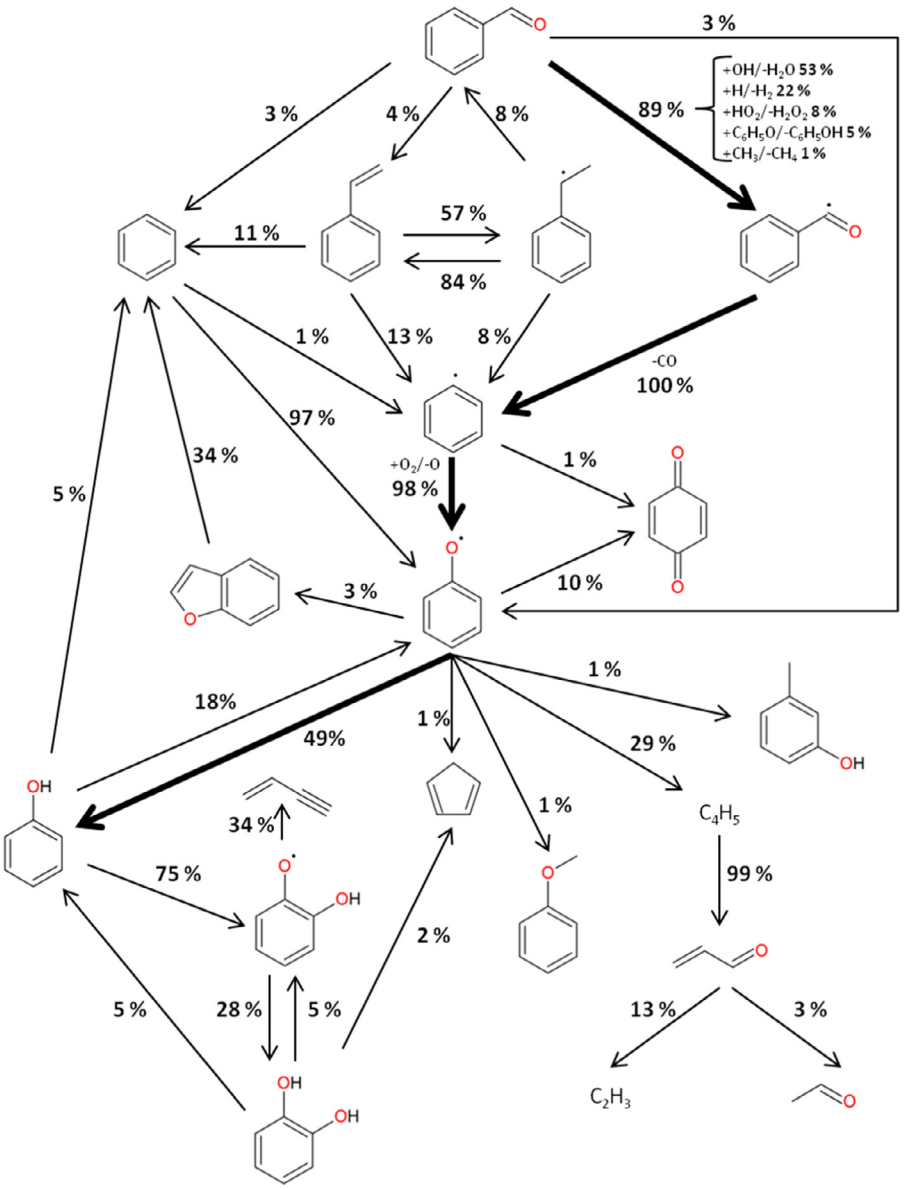

Fig. 6. Rate of production analysis at 850 K and 107 kPa of benzaldehyde oxidation under stoichiometric conditions. Percentages represent the fraction of the molar flux of consumption of the associated species.

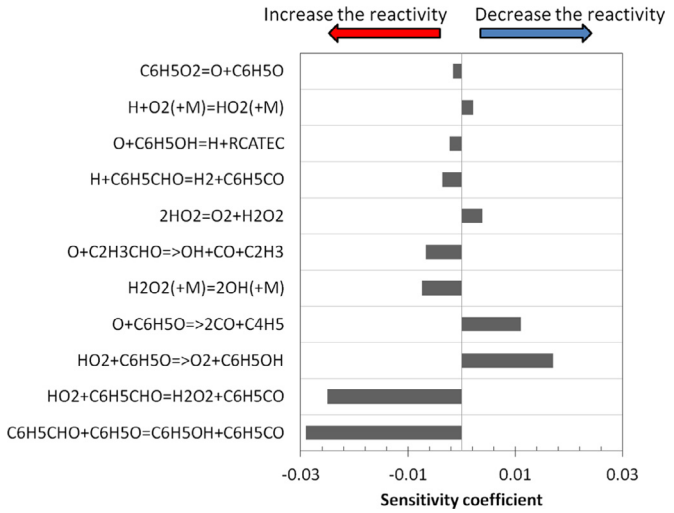

Fig. 7. Sensitivity analysis of benzaldehyde oxidation to rate constants at $T = 770$ K and $\varphi = 1$.

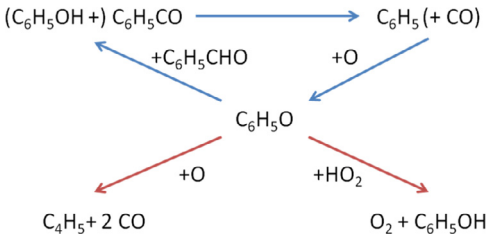

Fig. 8. Scheme of the phenoxy radical reactions implied in the control of the overall reactivity of the system (in blue the accelerating propagating chain loop and in red the inhibiting reactions).

tion: $C_2H_3+O_2=H+CO+CH_2O$. The non-detection of formaldehyde during the experiment may indicate that the transformation of acrolein into C_2H_3 and acetaldehyde needs a better assessment.

Concerning the simulated profiles of catechol, its formation is due to the ipso-addition reaction of an oxygen atom on phenol. This leads to the formation of the resonance stabilized phenoxy-like catechol radical, which can then react with other species in

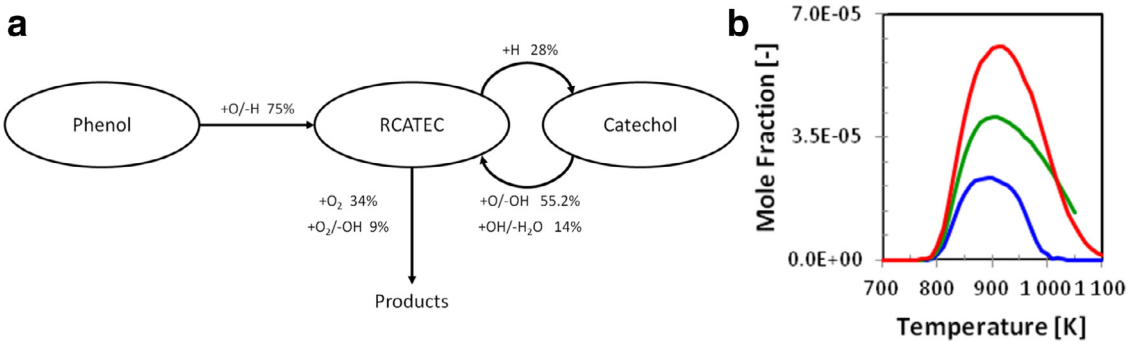

Fig. 9. (a) Flux rate between phenol and catechol at 850 K and (b) simulation data for catechol obtained with the kinetic model.

the system abstracting an H atom and forming catechol as shown in Fig. 9a).

The importance of such pathways in oxygenated aromatics has been recently pointed out by Pelucchi et al. [7]. The model predicts a fraction of catechol between 60 ppm under fuel-rich conditions and 25 ppm under fuel-lean conditions. A chart in Fig. 9b) presents the simulations results for catechol.

Despite this consideration the relative small amount of catechol predicted could lead to a more limited detection capability. Further analysis with gas chromatography and *ad hoc* analytical methods could help us to detect catechol in the outlet mixture.

5. Conclusion

In this work, benzaldehyde oxidation was investigated for the first time. Using a JSR coupled with gas chromatographs, 48 compounds were identified for various equivalence ratios covering from fuel lean to rich conditions. 28 mol fraction profiles were obtained for species from major ones (CO, CO_2, phenol) to some minor products (acrolein, acetaldehyde, benzene, cresol, etc.), other species being present in the form of traces. These new data were compared with simulation results obtained with an updated version of the CRECK kinetic model. The model update allowed for a better description of benzaldehyde oxidation. The decomposition of benzaldehyde mainly leads to the formation of phenyl radical which then oxidize to give phenoxy radical (C_6H_5O), ruling the formation of almost all the observed products. Another relevant reaction class is that of ipso-addition reactions leading to the formation of benzene and phenol, directly from benzaldehyde. Those compounds also react to give the C_6H_5O radical. The updated CRECK kinetic model provides a valuable starting point for further refinement towards a more systematic characterization of oxygenated functional groups effect on substituted aromatics kinetics of interest for bio-oils combustion applications.

This work confirms the importance of the C_6H_5O radical in the decomposition of oxygenated aromatic compounds and provides a first detailed assessment of benzaldehyde oxidation kinetics upon which more accurate kinetic subsets should be developed.

Declaration of Competing Interest

The authors declare that they have no known competing financial interests or personal relationships that could have appeared to influence the work reported in this paper.

Acknowledgments

This work has received funding from the European Union H2020 (H2020-SPIRE-04–2016) under grant agreement n° 723706 and from the COST Action CM1404 “Chemistry of smart energy carriers and technologies”.

Supplementary materials

Supplementary material associated with this article can be found, in the online version, at doi:10.1016/j.combustflame.2019.09.024.

References

[1] N. Sebbar, J.W. Bozzelli, H. Bockhorn, Thermochemistry and reaction paths in the oxidation reaction of benzoyl radical: C6H5C•(=O), J. Phys. Chem. A. 115 (2011) 11897–11914, doi:10.1021/jp2078067.
[2] W. Pejpichestakul, E. Ranzi, M. Pelucchi, A. Frassoldati, A. Cuoci, A. Parente, T. Faravelli, Examination of a soot model in premixed laminar flames at fuel-rich conditions, Proc. Combust. Inst. (2018), doi:10.1016/j.proci.2018.06.104.
[3] M. Pelucchi, C. Cavallotti, T. Faravelli, S.J. Klippenstein, H-Abstraction reactions by OH, HO2, O, O2 and benzyl radical addition to O2 and their implications for kinetic modelling of toluene oxidation, Phys. Chem. Chem. Phys. 20 (2018) 10607–10627, doi:10.1039/C7CP07779C.
[4] B. Husson, M. Ferrari, O. Herbinet, S.S. Ahmed, P.-.A. Glaude, F. Battin-Leclerc, New experimental evidence and modeling study of the ethylbenzene oxidation, Proc. Combust. Inst. 34 (2013) 325–333, doi:10.1016/j.proci.2012.06.002.
[5] M. Bertero, G. de la Puente, U. Sedran, Fuels from bio-oils: bio-oil production from different residual sources, characterization and thermal conditioning, Fuel. 95 (2012) 263–271, doi:10.1016/j.fuel.2011.08.041.
[6] L. Negahdar, A. Gonzalez-Quiroga, D. Otyuskaya, H.E. Toraman, L. Liu, J.T.B.H. Jastrzebski, Kevin.M.Van Geem, G.B. Marin, J.W. Thybaut, B.M. Weckhuysen, Characterization and comparison of fast pyrolysis bio-oils from pinewood, rapeseed cake, and wheat straw using 13C NMR and comprehensive GC × GC, ACS Sustain. Chem. Eng. 4 (2016) 4974–4985, doi:10.1021/acssuschemeng.6b01329.
[7] M. Pelucchi, C. Cavallotti, A. Cuoci, T. Faravelli, A. Frassoldati, E. Ranzi, Detailed kinetics of substituted phenolic species in pyrolysis bio-oils, React. Chem. Eng. 4 (2019) 490–506, doi:10.1039/C8RE00198G.
[8] A.K. Vasiliou, J.H. Kim, T.K. Ormond, K.M. Piech, K.N. Urness, A.M. Scheer, D.J. Robichaud, C. Mukarakate, M.R. Nimlos, J.W. Daily, Q. Guan, H.-.H. Carstensen, G.B. Ellison, Biomass pyrolysis: thermal decomposition mechanisms of furfural and benzaldehyde, J. Chem. Phys. 139 (2013) 104310, doi:10.1063/1.4819788.
[9] M. Nowakowska, O. Herbinet, A. Dufour, P.-.A. Glaude, Detailed kinetic study of anisole pyrolysis and oxidation to understand tar formation during biomass combustion and gasification, Combust. Flame. 161 (2014) 1474–1488, doi:10.1016/j.combustflame.2013.11.024.
[10] H. Wang, Formation of nascent soot and other condensed-phase materials in flames, Proc. Combust. Inst. 33 (2011) 41–67, doi:10.1016/j.proci.2010.09.009.
[11] C.D. Hurd, C.W. Bennett, The pyrolysis of benzaldehyde and of benzyl benzoate, J. Am. Chem. Soc. 51 (1929) 1197–1201, doi:10.1021/ja01379a030.
[12] R. Solly, S. Benson, Kinetics of gas-phase unimolecular decomposition of benzoyl radical, J. Am. Chem. Soc. 93 (1971) 2127, doi:10.1021/ja00738a006.
[13] M. Grela, A. Colussi, Kinetics and mechanism of the thermal-decomposition of unsaturated aldehydes - Benzaldehyde, 2-Butenal, and 2-Furaldehyde, J. Phys. Chem. 90 (1986) 434–437, doi:10.1021/j100275a016.
[14] O.S.L. Bruinsma, R.S. Geertsma, P. Bank, J.A. Moulijn, Gas phase pyrolysis of coal-related aromatic compounds in a coiled tube flow reactor: 1. benzene and derivatives, Fuel 67 (1988) 327–333, doi:10.1016/0016-2361(88)90314-6.
[15] N. Vin, O. Herbinet, F. Battin-Leclerc, Diethyl ether pyrolysis study in a jet-stirred reactor, J. Anal. Appl. Pyrolysis. 121 (2016) 173–176, doi:10.1016/j.jaap.2016.07.018.
[16] O. Herbinet, F. Battin-Leclerc, Progress in understanding low-temperature organic compound oxidation using a jet-stirred reactor, Int. J. Chem. Kinet. 46 (2014) 619–639, doi:10.1002/kin.20871.
[17] W.K. Metcalfe, S.M. Burke, S.S. Ahmed, H.J. Curran, A hierarchical and comparative kinetic modeling study of C1− C2 hydrocarbon and oxygenated fuels, Int. J. Chem. Kinet. 45 (2013) 638–675.

[18] S.M. Burke, U. Burke, R. Mc Donagh, O. Mathieu, I. Osorio, C. Keesee, A. Morones, E.L. Petersen, W. Wang, T.A. DeVerter, M.A. Oehlschlaeger, B. Rhodes, R.K. Hanson, D.F. Davidson, B.W. Weber, C.-J. Sung, J. Santner, Y. Ju, F.M. Haas, F.L. Dryer, E.N. Volkov, E.J.K. Nilsson, A.A. Konnov, M. Alrefae, F. Khaled, A. Farooq, P. Dirrenberger, P.-A. Glaude, F. Battin-Leclerc, H.J. Curran, An experimental and modeling study of propene oxidation. part 2: ignition delay time and flame speed measurements, Combust. Flame. 162 (2015) 296–314, doi:10.1016/j.combustflame.2014.07.032.

[19] E. Ranzi, A. Frassoldati, R. Grana, A. Cuoci, T. Faravelli, A.P. Kelley, C.K. Law, Hierarchical and comparative kinetic modeling of laminar flame speeds of hydrocarbon and oxygenated fuels, Prog. Energy Combust. Sci. 38 (2012) 468–501, doi:10.1016/j.pecs.2012.03.004.

[20] E. Ranzi, A. Frassoldati, A. Stagni, M. Pelucchi, A. Cuoci, T. Faravelli, Reduced kinetic schemes of complex reaction systems: fossil and biomass-derived transportation fuels, Int. J. Chem. Kinet. 46 (2014) 512–542, doi:10.1002/kin.20867.

[21] B. Ruscic, Uncertainty quantification in thermochemistry, benchmarking electronic structure computations, and active thermochemical tables, Int. J. Quantum Chem. 114 (2014) 1097–1101, doi:10.1002/qua.24605.

[22] A. Burcat, B. Ruscic, Chemistry, T.-I.I. of Tech, Third millennium ideal gas and condensed phase thermochemical database for combustion (with update from active thermochemical tables), Argonne National Lab. (ANL), Argonne, ILUnited States, 2005, doi:10.2172/925269.

[23] C. Muller, V. Michel, G. Scacchi, G.M. Côme, THERGAS: a computer program for the evaluation of thermochemical data of molecules and free radicals in the gas phase, J. Chim. Phys. Phys.-Chim. Biol. 92 (1995) 1154–1178.

[24] S.W. Benson, F.R. Cruickshank, D.M. Golden, G.R. Haugen, H.E. O'Neal, A.S. Rodgers, R. Shaw, R. Walsh, Additivity rules for the estimation of thermochemical properties, Chem. Rev. 69 (1969) 279–324, doi:10.1021/cr60259a002.

[25] M. Pelucchi, S. Namysl, E. Ranzi, A. Frassoldati, O. Herbinet, F. Battin-Leclerc, T. Faravelli, An experimental and kinetic modelling study of n-C4C6 aldehydes oxidation in a jet-stirred reactor, Proc. Combust. Inst. 37 (2019) 389–397, doi:10.1016/j.proci.2018.07.087.

[26] R. Bounaceur, I. Da Costa, R. Fournet, F. Billaud, F. Battin-Leclerc, Experimental and modeling study of the oxidation of toluene, Int. J. Chem. Kinet. 37 (2005) 25–49, doi:10.1002/kin.20047.

[27] C. Saggese, A. Frassoldati, A. Cuoci, T. Faravelli, E. Ranzi, A wide range kinetic modeling study of pyrolysis and oxidation of benzene, Combust. Flame. 160 (2013) 1168–1190, doi:10.1016/j.combustflame.2013.02.013.

[28] Y. Zhang, K.P. Somers, M. Mehl, W.J. Pitz, R.F. Cracknell, H.J. Curran, Probing the antagonistic effect of toluene as a component in surrogate fuel models at low temperatures and high pressures. a case study of toluene/dimethyl ether mixtures, Proc. Combust. Inst. 36 (2017) 413–421, doi:10.1016/j.proci.2016.06.190.

[29] J. Mendes, C.-.W. Zhou, H.J. Curran, Theoretical chemical kinetic study of the H-Atom abstraction reactions from aldehydes and acids by Ḣ atoms and ȮH, HȮ2, and ĊH3 radicals, J. Phys. Chem. A. 118 (2014) 12089–12104, doi:10.1021/jp5072814.

[30] A. Cuoci, A. Frassoldati, T. Faravelli, E. Ranzi, OpenSMOKE++: an object-oriented framework for the numerical modeling of reactive systems with detailed kinetic mechanisms, Comput. Phys. Commun. 192 (2015) 237–264, doi:10.1016/j.cpc.2015.02.014.

[31] M. Lubrano Lavadera, Y. Song, P. Sabia, O. Herbinet, M. Pelucchi, A. Stagni, T. Faravelli, F. Battin-Leclerc, M. de Joannon, Oscillatory behavior in methane combustion: influence of the operating parameters, Energy Fuels 32 (2018) 10088–10099, doi:10.1021/acs.energyfuels.8b00967.